

NOVEL SYNTHESIS, PROPERTIES, AND STRUCTURAL CHARACTERISTICS OF 1,6-DIALKYLPIRIMIDO[5,4-*e*][*n*](2,4)-PYRIDINOPHANE-5,7(1*H*,6*H*)-DIONES

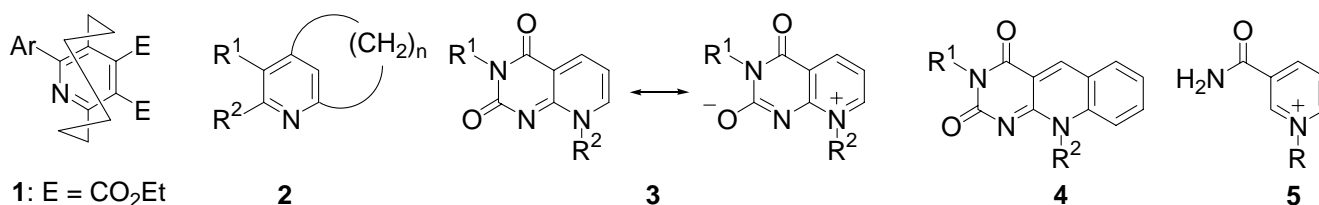
Makoto Nitta,* Hiromi Kanda, Hiroyuki Yamamoto, and Shin-ichi Naya

Department of Chemistry, School of Science and Engineering, Waseda University, Shinjuku-ku, Tokyo 169-8555, Japan

Abstract - Novel synthesis of the 1,6-dialkylpyrimido[5,4-*e*][*n*](2,4)pyridinophane-5,7(1*H*,6*H*)-diones ($n = 11, 9, 6$) (5,7-polymethylene-substituted 8-alkylpyrido[2,3-*d*]pyrimidine-2,4(3*H*,8*H*)-diones) consists of allowing 3-methyl-6-benzylaminouracil to react with cycloalk-2-enones. Their chemical and electrochemical properties as well as structural characteristics are studied on the basis of their spectroscopic properties, cyclic voltammetry, X-Ray analysis, and theoretical calculations. Deformation of the pyridine ring of a [6](2,4)pyridinophane derivative is observed by X-Ray analysis. Furthermore, isolation of a dihydrogenated [5](2,4)pyridinophane derivative and its unsuccessful dehydrogenation reaction leading to the first example of a [5](2,4)pyridinophane derivative are investigated as well.

INTRODUCTION

The remarkable chemical and physical properties of strained cyclophanes continue to fascinate many organic chemists.¹⁻⁴ In the field of heterocyclic[*n*]paracyclophanes,^{5,6} the smallest known member is [6](2,5)pyridinophane (**1**).⁵ In the [*n*]metacyclophane series, the smallest known members thus far synthesized are 3-halogeno[6](2,4)pyridinophane,⁷ [n](2,6)pyridinophanes ($n = 12$ and $n = 10-6$),⁸

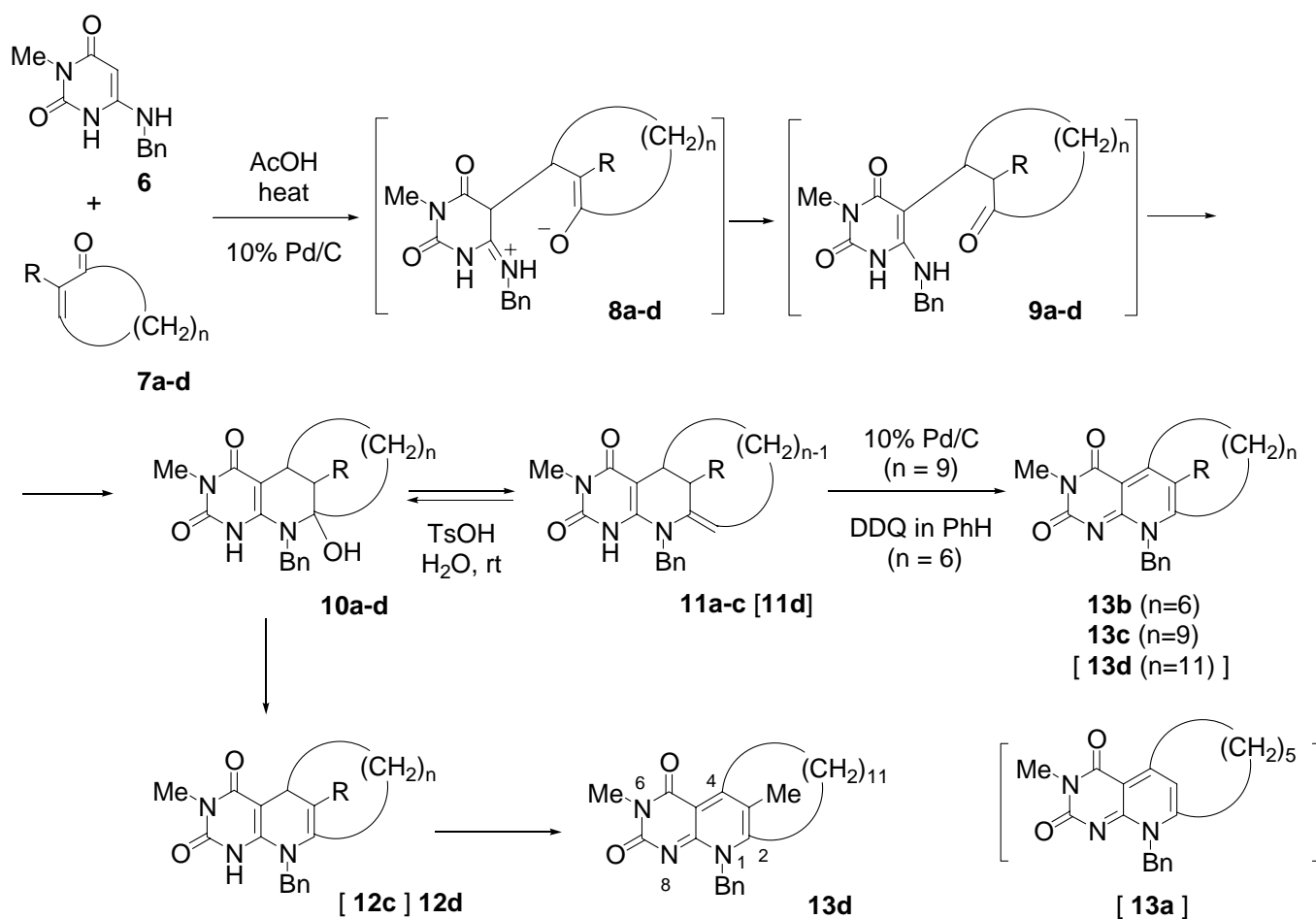


Scheme 1

[n](3,5)pyridinophanes (n = 9 and 7),⁹ and 3-chloro[6](2,4)quinolinophane.^{10,11} Previously, we have also worked on convenient preparations of a series of [n](2,4)pyridinophanes (n = 9-6) (**2**),¹² azulenoannulated [n](2,4)pyridinophanes (n = 9-6),¹³ [n](2,4)quinolinophanes (n = 9-7),¹⁴ and dimethyluracilannulated [n](2,4)pyridinophanes (n = 9-6),¹⁵ and studied their static and dynamic behaviors. The synthesis consists of an enamine alkylation process of vinyliminophosphoranes,^{12,16} 2-aminoazulenes,¹³ β -aminoenones,¹⁴ and 6-amino-1,3-dimethyluracil¹⁵ with cycloalk-2-enones, respectively, and subsequent condensation of the nitrogen moiety with the carbonyl function and dehydrogenation. Thus, a few easy reaction steps enable the synthesis of novel and highly interesting types of condensed heterocycles, which are difficult to obtain by other synthetic means.¹⁶ 8-Alkylpyrido[2,3-*d*]pyrimidine-2,4(3*H*,8*H*)-dione (**3**) is interesting in view of their structural characteristics as they have a conjugated system similar to that of 5-deazaflavin (**4**), which has been studied extensively in both enzymatic and model systems in the hope of providing mechanistic insight into flavin-catalyzed reactions,¹⁷⁻¹⁹ and one of the canonical structures can be considered as an NAD(P)⁺ model (**5**). In this context, as well as to pursue our interest in enzymatic or catalytic functions, we have studied a new facile synthesis, the chemical and electrochemical properties, and the structural characteristics of novel 1,6-alkylpyrimido[5,4-*e*][n](2,4)pyridinophan-5,7(1*H*,6*H*)-diones (**11a-d**) (5,7-polymethylene-substituted 8-alkylpyrido[2,3-*d*]pyrimidine-2,4(3*H*,8*H*)-diones). We report herein the results in detail.

RESULTS AND DISCUSSION

Thermal reaction of 3-methyl-6-benzylaminouracil (**6**) with cycloalk-2-enones (**7a**) (R = H, n = 5) and (**7b**) (R = H, n = 6) was examined in AcOH in the presence of a catalytic amount of a dehydrogenating agent (10% Pd/C) under reflux to give alcohol (**10a**) and dehydrated products (**11a**) and (**11b**), respectively (Scheme 2). The reaction conditions and the yields of the products are summarized in Table 1 (Runs 1 and 2). On the other hand, the reaction of **6** with **7c** (R = H, n = 9) and **7d** (R = Me, n = 11) under similar conditions afforded [9] and [11](2,4)pyridinophane derivatives, 1-benzyl-6-methylpyrimido[5,4-*e*][n](2,4)pyridinophane-5,7(1*H*,6*H*)-diones (n = 9 and 11) (**13c**) and (**13d**), respectively (Table 1, Runs 3 and 4). The postulated mechanistic pathways for the formation of alcohol (**10a**) and its dehydrated compounds (**11a,b**) as well as pyridinophane derivatives (**13c,d**) are also shown in Scheme 2. Enamine alkylation of **6** to the β -carbon atom of **7a-d** gives zwitterions (**8a-d**). The following tautomerization in **8a-d** regenerates the β -aminoenone moiety in **9a-d**. The enamine intermediates (**9a-d**) undergo an intramolecular attack to produce hydroxylated products (**10a-d**). In the case of the highly constrained **10a** (n = 5), it undergoes partial dehydration to lead to **11a**, and thus, both **10a** and **11a** are isolated. In the case of **10b** (n = 6), dehydration occurs more easily, as compared



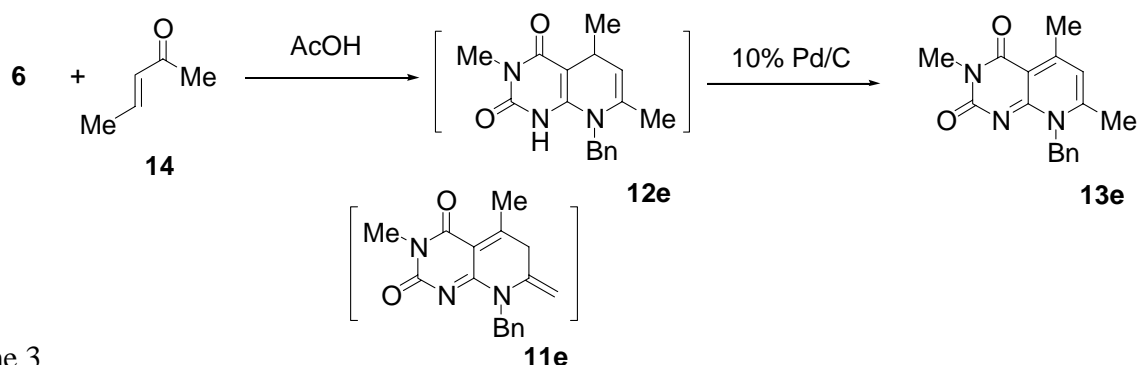
Scheme 2

Table 1. Results for the reactions of **6** with **7a-e**^a

Run	Alkenone (Yield/%) ^b	n	R	Molar ratio	Reaction	Product 7/6	Time/h
1	7a	5	H	1.2	7	10a (56), 11a (40)	
2	7b	6	H	1.2	4	11b (96)	
3	7c	9	H	1.2	6	13c (56)	
4	7d	11	Me	1.2	16	13d (30)	
5	14	---	---	1.2	6	13e (62)	

a. Reaction was carried out in AcOH under reflux. b. Isolated yield.

with **10a** (n = 5), to result in the formation of **11b**. Compounds (**11a,b**) do not undergo dehydrogenating aromatization leading to [5] and [6](2,4)pyridinophane derivatives (**13a,b**) in the presence of 10% Pd/C. On the other hand, less constrained **10c,d** undergo dehydration easily to give **11c,d**, which undergo dehydrogenative aromatization in the presence of 10% Pd/c to result in the formation of [9] and [11](2,4)pyridinophane derivatives (**13c,d**). An alternative possibility for



Scheme 3

dehydration of **9c,d** would be the formation of **12c,d**, which are dehydrogenated by 10% Pd/C to give **13c,d**. 1,4-Dihydropyridines such as **12c,d** have been postulated in the previous papers, and 1,4-dihydro[6](2,4)pyridinophane is isolated.¹⁴ In order to confirm this aspect, the heat of formation (ΔH_f°) for **11a-e** and **12a-e** (cf. Scheme 3) was calculated by the MOPAC Ver 6.12 program and the results are listed in Table 2. The calculated results suggest that compounds (**11a-c**) are more stable than **12a-c**, while compounds (**12d,e**) are more stable than **11d,e**. This is probably due to the less constrained nature of the 1,4-dihydropyridine ring system such as **12d** and **12e** as compared with **12a-c**. Thus, the intermediate (**12d**) seems to be preferable for the formation of (11)[2,4]pyridinophane derivative (**13d**). In a similar fashion to the pyridinophane synthesis, thermal reaction of **6** with 3-penten-2-one (**14**) in the presence of a dehydrogenating agent (10% Pd/C) under reflux in AcOH afforded compound (**13e**) in moderate yield (Table 1, Run 5). In this case, the intermediate (**12e**) is suggested to be more stable than **11e** (Table 2), and thus, **12e**, as in the case of **12d**, is the plausible intermediate. Furthermore, independent dehydrogenation of **11b** with DDQ afforded constrained [6](2,4)pyridinophane-type compounds (**13b**), while attempted dehydrogenation of highly constrained **11a** with DDQ, NiO₂, or MnO₂ could not afford **13a** and gave only unidentified materials. In addition, in the acid (TsOH)-catalyzed hydration of the constrained double bond, 57% of **11a** was converted to

Table 2. Calculated heat of formation ($\Delta H_f^\circ / \text{kcalmol}^{-1}$) of **11a-e** and **12a-e**

	$\Delta H_f^\circ / \text{kcalmol}^{-1}$	
	11a-e	12a-e
a (n=5)	-6.38	-3.44
b (n=6)	-11.02	-6.20
c (n=9)	-34.80	-35.25
d (n=11)	-48.46 (<i>trans</i>) -25.31 (<i>cis</i>)	-54.41
e (Me ₂)	-0.27	-3.03

Table 3. ¹H NMR spectral data of **13b-d** and reference compound **13e**^a

Compd.	δ (H6)	δ (H1' and Hn')	Remaining signals
13b	6.73 (s)	2.65-2.71 (1H, m) 2.76-2.82 (1H, m) 2.93-2.98 (1H, m) 4.38 (1H, quin, <i>J</i> 5.7)	0.51 (1H, br s), 0.60 (1H, br s), 1.05-1.12 (1H, m), 1.21-1.30 (1H, m), 1.39-1.42 (1H, m), 1.50-1.58 (1H, m), 1.77 –1.85 (1H, m), 5.64 (1H, d, <i>J</i> 5.5), 5.81 (1H, d, <i>J</i> 5.5), 7.23 (2H, d, <i>J</i> 7.2), 7.31 (1H, <i>J</i> 7.2), 7.34 (1H, d, <i>J</i> 7.2)
13c	6.72 (s)	2.84 (2H, t, <i>J</i> 6.3) 3.41 (2H, t, <i>J</i> 5.9)	1.06-1.34 (10H, m), 1.77 (1H, quint, <i>J</i> 6.3), 1.93 2H, quint, <i>J</i> 5.9), 3.43 (3H, s), 5.90 (2H, br s), 7.07 (2H, d, <i>J</i> 6.8), 7.22-7.34 (3H, m)
13d	--	2.75 (1H, dq, <i>J</i> 6.1, 3.9) 2.90-3.07 (2H, m) 4.93 (1H, dq, <i>J</i> 6.1, 3.9)	0.65-1.02 (5H, m), 1.02-1.50 (9H, m), 1.50-1.90 (4H, m), 2.34 (3H, s), 3.44 (3H, s), 5.03 (2H, br s), 7.05 (2H, d, <i>J</i> 6.8), 7.22-7.34 (3H, m),
13e	6.48 (s)	2.48 (3H, s) 2.43 (3H, s)	5.87 (2H, br s), 7.09 (2H, br d), 7.22-7.34 (3H, m)

a. Recorded on a 600 MHz spectrometer.

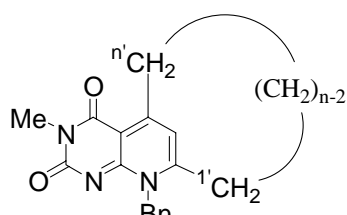


Figure 1.

10a. The structures of compounds (**10a**), (**11a,b**), and (**13b-d**) were deduced from their spectral data and elemental analyses. The ¹H NMR spectral data for [n](2,4)pyridinophane derivatives (**13b-d**) as well as reference compound (**13e**) are summarized in Table 3 (see the convenient, but not systematic numbering of the methylene illustrated in Figure 1). A characteristic feature of **13c** is the equivalence of the geminal hydrogens at the 'benzylic' positions H1' and H9' (Figure 1), where the signals appear as a couple of triplets. This feature is indicative of a rapid flipping of the methylene bridge of **13c** at room temperature; and spectral properties similar to those of **13c** were also observed for [9](2,4)pyridinophane derivatives' which undergo rapid flipping.¹²⁻¹⁴ In contrast, the four benzylic hydrogens of **13b** and **13d** exhibited different chemical shifts at room temperature (Table 3), suggesting that the flipping of the constrained hexamethylene chain and the undecamethylene chain, which is sterically hindered due to the methyl group at C3, are frozen in the NMR time scale at room temperature. The UV spectra of pyridinophane (**13b-d**) are summarized in Table 4. The spectra of **13b-d** are similar, but the absorption maxima of **13d** are shifted to longer wave-lengths than those of **13b,c** probably due to the methyl group at the C3 position. On the other hand, the longest absorption maximum of **13b** is shifted slightly to a longer wave-length than that of **13c**, because of the short hexamethylene chain.¹²⁻¹⁵ The redox

Table 4. UV Spectral Data of **13b-d** and reference compound (**13e**)

Compd.	n	λ_{\max} /nm (log ϵ) (MeCN)			
13b	6	376 (3.65),			238 (3.67)
13c	9	374 (4.00),	275 (3.90),	257sh (4.05),	242 (4.12)
13d	11	381 (3.97),	278 (3.39),	258sh (4.10),	244 (4.06)
13e	--	368 (4.06),	274 (3.93),	257 (4.09),	225sh (4.23)

Table 5. Redox potentials^a of **13b-e** and reference compound (**4**), and the energy levels of LUMO and HOMO of **13b-e**

Compd.	E_{red}	E_{ox}	LUMO/eV	HOMO/eV
13b	-1.96	1.24	-0.999	-8.854
13c	-1.99	1.37	-1.030	-8.999
13d	-2.03	1.20	-1.053	-8.812
13e	-2.00	1.33	-1.104	-8.991
4^b	-1.42	---	---	---

a. Peak potential in V vs Ag/AgNO₃. b. Ref. 20

potentials of **13b-e** were determined by cyclic voltammetry (CV) in CH₃CN. The redox waves are irreversible under the conditions of CV measurement; the peak potentials of **13b-e** and reference compound (**4**; R¹ = Me, R² = dodecyl) are summarized in Table 5 together with the energy levels of the LUMO and HOMO predicted by AM1 calculations (MOPAC Ver 6.12). The E_{red} of **13b** is slightly more positive than those of less constrained **13c** and **13d,e**, although the LUMO of **13b** is slightly higher than those of **13c-e**, while the E_{ox} of **13b** is less positive than those of **13c,e**, reflecting the higher HOMO of **13b**. The E_{red} of **13d**, which has an additional methyl group at C3, is more negative than those of **13b,c,e** and the E_{ox} is less positive than those of **13b,c,e**. The E_{red} of **4** (R¹ = Me, R² = dodecyl) is -1.42 V (Table 5),²⁰ and thus, the oxidizing ability of **13b-d** as well as **13e** would be lower than that of deazaflavin derivatives. Since deazaflavin derivatives are known to oxidize several alcohols and amines in an autorecycling process under aerobic conditions, we have investigated the oxidizing reaction of benzyl alcohol with **13c** under thermal and aerobic conditions; however, benzaldehyde was not obtained and the alcohol was recovered.

The structural details of 8-carboxy[6]paracyclophane have been reported on the basis of X-Ray analysis, which was performed at -150 °C.²¹ We performed the structure determination of **13b** and reference compound (**13e**) at -150 °C. The X-Ray crystal analysis revealed that **13b** exhibits two structures (**13b-I**) and (**13b-II**) in the solid state due to the difference in the conformation of the benzyl group. As

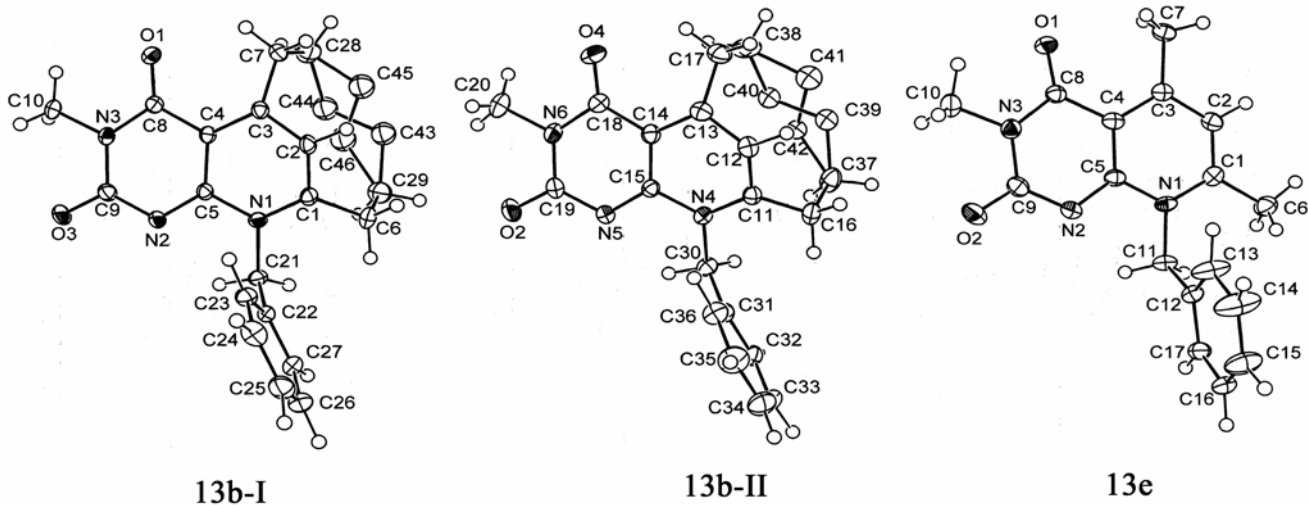


Figure 2

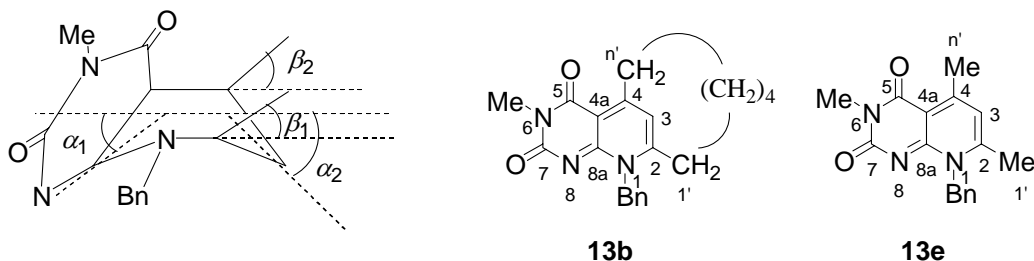


Figure 3

shown in Figures 2, the structure of **13b** is disordered, consisting of two conformers arising from the pseudo-rotation of the hexamethylene chain. Since it is therefore difficult to discuss the structure of the bridge-methylene in detail, we consider here mainly the structure of the pyridine ring. The selected bond lengths and angles of **13b-I**, **13b-II**, and **13e** are listed in Tables 6 and 7. Their values are similar. Thus, the bond lengths and angles of the pyridine ring of **13b** are not affected by the short hexamethylene chain. The most remarkable structural feature of **13b** is the deformation of the pyridine ring from planarity, which is represented by the deviation angles of the *para* carbons C8a and C3 (α_1 and α_2) from the base plane of the boat-shaped pyridine ring and those of the benzylic carbons C1' and Cn' (β_1 and β_2) from the bow of the pyridine ring as shown in Figure 3. The α_1 value is derived from the mean value of the torsion angles of C2-N1-C4a-C8a and C4-C4a-N1-C8a, and the α_2 value is derived from the mean value of the torsion angles of C4a-C4-C2-C3 and N1-C2-C4-C3. The β_1 value is derived from the mean value of the torsion angles of C1'-C2-C4-N1 and C1'-C2-C4-C4a, and the β_2 value is derived from the mean value of the torsion angles of Cn'-C4-C2-N1 and Cn'-C4-C2-C4a. These deformation angles of **13b** are remarkably larger than those of **13e** (Table 8). Thus, the feature suggests that the deformation of **13b** arises from the short hexamethylene chain. The bent angles of C3 (α_2) are larger

than those of C8a (α_1). In addition, the deviation angles (β_1 and β_2) of benzylic carbons C1' and Cn' are larger than the bent angles of C3 (α_2) and C8a (α_1). The feature suggests that the strains of pyridinophanes having a short methylene bridge cause a substantial deformation of benzylic carbons C1' and Cn'.

Table 6. Selected bond length of **13b** and **13e** obtained by X-Ray structure analysis

Compd.	Bond length ^a						
	N1-C8a	C8a-C4a	C4-C4a	C3-C4	C2-C3	C2-N1	C8a-N8
13b-I	1.390	1.423	1.386	1.406	1.366	1.364	1.319
13b-II	1.387	1.418	1.394	1.401	1.377	1.371	1.330
13e	1.400	1.411	1.400	1.406	1.372	1.359	1.324

a. The numbering is shown in Figure 3.

Table 7. Selected bond angle of **13b** and **13e** obtained by X-Ray structure analysis

Compd.	Bond angle ^a / degree						
	N1-C8a-C4a	C8a-C4a-C4	C4a-C4-C3	C4-C3-C2	C3-C2-N1	C2-N1-C8a	C4a-C8a-N8
13b-I	117.2	119.7	117.8	119.4	119.4	121.1	125.8
13b-II	117.7	119.8	117.6	119.5	118.8	121.1	125.4
13e	117.9	121.2	117.4	121.8	120.1	121.5	126.3

a. The numbering is shown in Figure 3.

Table 8. Deformation angles^a (α_1 , α_2 , β_1 , and β_2 / degree) of **13b-I**, **13b-II**, and **13e**

Compd.	α_1	α_2	β_1	β_2
13b-I	11.5	19.5	36.5	32.3
13b-II	11.1	20.4	34.9	36.2
13e	4.1	1.3	2.1	1.5

a. Shown in Figure 3.

EXPERIMENTAL

IR spectra were recorded on a Horiba FT-710 spectrophotometer. UV-VIS spectra were recorded on a Shimadzu UV-3101PC spectrophotometer. MS and HRMS (FAB) were run on JEOL JMS-AUTOMASS150 and JMS-SX102A spectrometers. Unless otherwise specified, ^1H and ^{13}C NMR

spectra were recorded on JNM-AL 400 and AVANCE600 spectrometers using CDCl_3 as a solvent, and the chemical shifts are given relative to internal SiMe_4 standard; J -values are given in Hz. Mps were recorded on a Yamato MP-21 apparatus and are uncorrected. All reactions except hydrolysis were carried out under anhydrous conditions and dry nitrogen atmosphere.

Preparation of 10a, 11a, and 11b. A solution of **6** (203 mg, 1 mmol) and **7a,b** (1.2 mmol) in AcOH (5 mL) was heated under reflux for the period indicated in Table 1. After the reaction mixture was concentrated, the residue was recrystallized from EtOH to give the products. The isolated yields are summarized in Table 1.

For **10a**: colorless powder; mp 176-177 °C (from CH_2Cl_2); ^1H NMR (400 MHz; $\text{DMSO}-d_6$) δ 1.00-1.27 (2H, m), 1.28-1.55 (3H, m), 1.55-1.81 (3H, m), 1.90-2.00 (1H, m), 2.42 (2H, br d, $J=14.4$ Hz), 2.68-2.80 (1H, m), 3.04 (3H, s), 4.82 (1H, d, $J=17.8$ Hz, PhCH), 4.90 (1H, d, $J=17.8$ Hz, PhCH), 5.90 (1H, s), 7.18 (2H, d, $J=7.3$ Hz), 7.22 (1H, d, $J=7.1$ Hz), 7.33 (2H, t, $J=7.6$ Hz), 9.61 (1H, br s); ^{13}C NMR (125.8 MHz; $\text{DMSO}-d_6$) δ 22.4, 23.8, 26.1, 27.0, 30.6, 32.5, 42.4, 85.0, 126.1, 126.2, 128.0, 139.0, 146.2, 150.7, 161.4; IR (KBr) 2929, 2854, 1689, 1600, 1471, 1394, 1349 cm^{-1} ; MS (m/z) 355 (M^+ , 18), 246 (100). Anal. Calcd for $\text{C}_{20}\text{H}_{25}\text{N}_3\text{O}_3$: C, 67.58; H, 7.09; N, 11.82. Found: C, 67.22; H, 6.81; N, 11.57.

For **11a**: colorless powder; mp 211-213 °C (from AcOEt); ^1H NMR (400 MHz) δ 0.83-0.95(1H, m), 1.17-1.56 (4H, m), 1.77-1.90 (2H, m), 1.98 (1H, dd, $J=3.4, 12.2$ Hz), 2.16-2.37 (1H, m), 3.06-3.16 (1H, m), 3.11 (3H, s), 3.22 (1H, dd, $J=3.4, 14.1$ Hz), 4.74 (1H, d, $J=18.0$ Hz), 5.06 (1H, d, $J=18.0$ Hz), 5.41 (1H, d, $J=7.8$ Hz), 7.15 (2H, d, $J=7.1$ Hz), 7.24-7.35 (3H, m), 9.69 (1H, br s); ^{13}C NMR (125.8 MHz) δ 26.4, 26.9, 27.2, 27.3, 32.1, 33.2, 34.2, 50.0, 92.9, 114.7, 125.8, 127.6, 128.9, 136.3, 139.8, 146.2, 152.1, 161.9; IR (KBr) 3321, 2925, 2854, 1701, 1593, 1517, 1473, 1452, 1382, 1367, 1350 cm^{-1} ; MS (m/z) 337 (M^+ , 15), 246 (100). Anal. Calcd for $\text{C}_{20}\text{H}_{23}\text{N}_3\text{O}_2$: C, 71.19; H, 6.87; N, 12.45. Found: C, 70.97; H, 6.89; N, 12.52.

For **11b**: colorless powder; mp 239-240 °C (from EtOH); ^1H NMR (400 MHz) δ 1.05-0.20 (1H, m), 1.38-1.65 (5H, m), 1.73-1.87 (2H, m), 1.93-2.12 (1H, m), 2.07 (1H, dd, $J=3.9, 12.7$ Hz), 2.12-2.25 (1H, m), 3.05-3.13 (1H, m), 3.07 (1H, dd, $J=2.4$ and 12.7 Hz), 3.17 (3H, s), 4.75 (1H, d, $J=18.3$ Hz), 5.06 (1H, d, $J=18.3$ Hz), 5.30 (1H, t, $J=8.5$ Hz), 7.13 (2H, d, $J=7.3$ Hz), 7.27 (1H, d, $J=7.3$ Hz), 7.34 (2H, t, $J=7.3$ Hz), 8.91 (1H, br s); ^{13}C NMR (125.8 MHz) 25.2, 26.5, 26.9, 27.4, 28.8, 30.2, 30.5, 30.9, 50.5, 90.7, 112.9, 125.5, 127.8, 129.2, 135.8, 139.1, 145.5, 151.4, 162.0; IR (KBr) 3225, 2922, 2849, 1692, 1663, 1634, 1617, 1520, 1472, 1387, 1370, 1357, 1170 cm^{-1} ; MS(m/z) 351 (M^+ , 59), 146 (100). Anal. Calcd for $\text{C}_{21}\text{H}_{25}\text{N}_3\text{O}_2$: C, 71.77; H, 7.17; N, 11.92. Found: C, 71.46; H, 7.40; N, 11.92.

Hydration of 11a. A solution of **11a** (61 mg, 0.18 mmol) and TsOH (1 mg) in a mixture of acetone (7 mL) and H₂O (1 mL) was stirred at rt for 48 h. After evaporation of the acetone, the residue was extracted with CH₂Cl₂ and the extract was dried over Na₂SO₄ and concentrated. The resulting residue was analyzed by ¹H NMR spectroscopy to reveal that 57% of **11a** was converted to **10a**.

Dehydrogenation of 11b. A solution of **11b** (21 mg, 0.06 mmol) and DDQ (16 mg, 0.07 mmol) in C₆H₆ (1 mL) was stirred at rt for 48 h. To the mixture was added NEt₃ and the mixture was concentrated. The resulting residue was purified by TLC on SiO₂ using AcOEt as the developing solvent to give **13b** in 30%.

For **13b**: colorless powder; mp 206-208 °C (from EtOH); ¹³C NMR (125.8 MHz) δ 26.6, 27.0, 27.9, 29.3, 29.7, 30.7, 32.0, 33.2, 33.4, 49.1, 76.5, 77.5, 109.2, 121.4, 128.1, 135.8, 156.3, 157.5, 157.7, 163.1, 163.4; IR (KBr) 2924, 2850, 1680, 1628, 1553, 1506, 1456, 1385 cm⁻¹; MS (*m/z*) 349 (M⁺, 100), 259 (100). HRMS Calculated for C₂₁H₂₃N₃O₂: 350.1868 (M+H). Found: 350.1870 (M⁺+1). Anal. Calcd for C₂₁H₂₂N₃O₂-1/2H₂O: C, 71.65; H, 5.41; N, 11.93. Found: C, 72.02; H, 6.74; N, 11.86.

Preparation of 13c-e. A mixture of **6** (203 mg, 1 mmol), **7c,d** (1.2 mmol) as well as **14** (1.2 mmol), and a dehydrogenating agent (10% Pd/C, 10 mg) in AcOH (5 mL) was heated under reflux for the period indicated in Table 1. After the reaction mixture was filtered through Celite and the filtrate was concentrated, the residue was separated by TLC in SiO₂ using AcOEt as the developing solvent to give the product. The isolated yields are summarized in Table 1.

For **13c**: yellow needles; mp 214-215 °C (from EtOH); ¹³C NMR (125.8 MHz) δ 24.3, 25.0, 25.4, 25.6, 26.0, 26.2, 26.4, 27.9, 33.3, 34.4, 49.1, 111.0, 117.7, 126.3, 127.8, 128.9, 135.0, 154.9, 157.0, 157.8, 162.2, 162.9; IR (KBr) 2933, 2861, 1683, 1632, 1540, 1506, 1472, 1457, 1420, 1308, 1267, 1207, 1188 cm⁻¹; MS (*m/z*) 391 (M⁺, 62), 300 (100). Anal. Calcd for C₂₄H₂₉N₃O₂: C, 73.63; H, 7.47; N, 10.73. Found: C, 73.30; H, 7.17; N, 11.03.

For **13d**: yellow powder; mp 220-222 °C (from AcOEt); ¹³C NMR (125.8 MHz) δ 15.9, 23.5, 23.7, 23.8, 25.6, 25.7, 25.7, 26.5, 26.6, 26.7, 28.1, 28.3, 30.1, 50.6, 111.9, 121.5, 126.3, 127.7, 129.0, 135.6, 155.2, 155.9, 156.7, 163.3, 163.9; IR (KBr) 2927, 2861, 1675, 1633, 1585, 1526, 1499, 1296, 1244, 1018 cm⁻¹; MS (*m/z*) 433 (M⁺, 100). Anal. Calcd for C₂₇H₃₅N₃O₂: C, 74.79; H, 8.14; N, 9.69. Found: C, 74.49; H, 8.17; N, 9.60.

For **13e** yellow needles; mp 232-234 °C (from EtOH); ¹³C NMR (125.8 MHz) δ 21.4, 22.9, 27.9, 49.7, 111.1, 117.4, 126.5, 127.9, 129.0, 134.4, 152.6, 157.1, 157.4, 159.1, 163.4; IR (KBr) 2957, 2925,

1683, 1632, 1553, 1506, 1453, 1374, 1207 cm^{-1} ; MS (m/z) 295 (M^+ , 19), 91 (100%) Anal. Calcd for $\text{C}_{17}\text{H}_{17}\text{N}_3\text{O}_2$: C, 69.14; H, 5.80; N, 14.23. Found: C, 69.03; H, 5.65; N, 14.11.

Attempted oxidation of benzyl alcohol with 13c. A mixture of **13c** (16 mg, 0.04 mmol) and benzyl alcohol (0.5 g, 4.6 mmol) was heated at 90 °C for 20 h under aerobic conditions. The reaction mixture was then purified by column chromatography on SiO_2 to give recovery of benzyl alcohol in 95% yield.

Cyclic voltammetry of 13b-e. The reduction and oxidation potentials of **13b-e** were determined by means of CV-27 voltammetry controller (BAS Co). A three-electrode cell was used, consisting of Pt working and counter electrodes and a reference Ag/AgNO_3 electrode. Nitrogen was bubbled through an acetonitrile solution (4 mL) of each compound (0.5 mmol dm^{-3}) and Bu_4NClO_4 (0.1 mol dm^{-3}) to deaerate it. The measurements were made at a scan rate of 0.1 V s^{-1} and the voltammograms were recorded on a WX-1000-UM-019 (Graphtec Co) X-Y recorder. Immediately after the measurements, ferrocene (0.1 mmol) ($E_{1/2} = +0.083$) was added as the internal standard, and the observed peak potentials were corrected with reference to this standard. The compounds exhibited no reversible wave: each of the potentials was measured through independent scan, and they are summarized in Table 5.

X-Ray structure determination. For **13b**. Yellow prisms, $\text{C}_{21}\text{H}_{23}\text{N}_3\text{O}_2$, $M=349.43$, triclinic, space group $P-1$, $a=9.2479(2)$, $b=12.2193(4)$, $c=15.8472(3)$ Å, $\alpha=99.429(3)$, $\beta=95.189(1)$, $\gamma=94.137(5)^\circ$, $V=1752.44(8)$ Å³, $Z=4$, $D_c=1.324 \text{ g cm}^{-3}$, crystal dimensions 0.70×0.50×0.10 mm. Data were measured on a Rigaku RAXIS-RAPID radiation diffractometer with graphite monochromated Mo- $K\alpha$ radiation. A total 15367 reflections were collected, using the ω - 2θ scan technique to a maximum 2θ value of 55.0. The structure was solved by direct methods and refined by a full-matrix least-squares method using SIR92 structure analysis software,²² with 511 variables and 7590 observed reflections [$I > 3.00\sigma(I)$]. The non-hydrogen atoms were refined anisotropically. The weighting scheme $w=[\sigma_c^2(F_0)+0.0100\times F_0^2]^{-1}$ gave satisfactory agreement analysis. The final R and R_w values were 0.073 and 0.153. The maximum peak and minimum peak in the final difference map were 0.87 and $-0.33\text{e}^-/\text{Å}^3$.

For **13e**. Yellow platelet, $\text{C}_{17}\text{H}_{17}\text{N}_3\text{O}_2$, $M=295.34$, triclinic, space group $P-1$, $a=6.8806(8)$, $b=9.395(2)$, $c=12.254(2)$ Å, $\alpha=68.530(4)$, $\beta=83.555(8)$, $\gamma=85.654(5)^\circ$, $V=732.0(2)$ Å³, $Z=2$, $D_c=1.340 \text{ g cm}^{-3}$, crystal dimensions 1.00×1.00×0.20 mm. Data were measured on a Rigaku RAXIS-RAPID radiation diffractometer with graphite monochromated Mo- $K\alpha$ radiation. A total 6321 reflections were collected,

using the ω - 2θ scan technique to a maximum 2θ value of 55.0°. The structure was solved by direct methods and refined by a full-matrix least-squares method using SIR92 structure analysis software,²² with 217 variables and 2615 observed reflections [$I > 3.00\sigma(I)$]. The non-hydrogen atoms were refined anisotropically. The weighting scheme $w = [\sigma_c^2(F_o) + 0.0100 \times F_o^2]^{-1}$ gave satisfactory agreement analysis. The final R and R_w values were 0.068 and 0.145. The maximum peak and minimum peak in the final difference map were 0.37 and $-0.30\text{e}^-/\text{\AA}^3$.

ACKNOWLEDGEMENTS

Financial support from Waseda University Grant for Special Research Project and 21COE "Practical Nano-Chemistry" from MEXT, Japan is gratefully acknowledged. We thank the Material Characterization Central Laboratory, Waseda University, for technical assistance with the spectral data, elemental analyses and X-ray analysis.

REFERENCES

1. The older literature has been reviewed: P. M. Keehn and S. M. Rosenfeld, *Cyclophanes*, Academic Press, New York, 1983.
2. Review on small cyclophanes: V. V. Kane, W. H. de Wolf, and F. Bickelhaupt, *Tetrahedron*, 1994, **50**, 4575.
3. Y. Tobe, *Topics in Current Chemistry*, 1994, **172**, 1.
4. G. J. Bodwell, *Angew. Chem., Int. Ed. Engl.*, 1996, **35**, 2085.
5. T. Kobayashi and M. Nitta, *Bull. Chem. Soc. Jpn.*, 1985, **58**, 3099.
6. (a) H. Gerlach and E. Huber, *Helv. Chim. Acta*, 1968, **51**, 2027; (b) N. Kanomata and T. Nakata, *Angew. Chem., Int. Ed. Engl.*, 1997, **36**, 1207.
7. D. Dhanak and C. B. Reese, *J. Chem. Soc., Perkin Trans. 1*, 1987, 2829.
8. K. Biemann, G. Büchi, and B. H. Walker, *J. Am. Chem. Soc.*, 1957, **79**, 5558; S. Fujita and H. Nozaki, *Bull. Chem. Soc. Jpn.*, 1971, **44**, 2827; K. Tamao, S. Kodama, T. Nakatsuka, Y. Kiso, and M. Kumada, *J. Am. Chem. Soc.*, 1975, **97**, 4405.
9. A. T. Balaban, *Tetrahedron Lett.*, 1968, 4643; 1978, 5055.
10. W. E. Parham, R. W. Davenport, and J. B. Biasotti, *Tetrahedron Lett.*, 1969, 557; W. E. Parham, K. B. Sloan, and J. B. Biasotti, *Tetrahedron*, 1971, **27**, 5767; W. E. Parham, D. C. Egberg, and S. S. Salgar, *J. Org. Chem.*, 1972, **37**, 3248.
11. W. E. Parham, R. W. Davenport, and J. B. Biasotti, *J. Org. Chem.*, 1970, **35**, 3775.
12. N. Kanomata and M. Nitta, *Tetrahedron Lett.*, 1988, **29**, 5957; *J. Chem. Soc., Perkin Trans. 1*, 1990,

1119.

13. H. Miyabara, T. Takayasu, and M. Nitta, *Heterocycles*, 1999, **51**, 983; *J. Chem. Soc., Perkin Trans. I*, 1999, 3199.
14. M. Nitta, T. Akie, and Y. Iino, *J. Org. Chem.*, 1994, **59**, 1309.
15. H. Yamamoto, H. Takeda, and M. Nitta, *Heterocycles*, 2000, **53**, 1891.
16. For recent reviews: (a) Y. G. Gololobov and L. F. Kasukhin, *Tetrahedron*, 1992, **48**, 1353; (b) S. Eguchi, Y. Matsushita, and K. Yamashita, *Org. Prep. Proced. Int.*, 1992, **24**, 209; (c) M. Nitta, *Reviews on Heteroatom Chem.*, 1993, **9**, 87; (d) P. Molina and M. J. Vilaplana, *Synthesis*, 1994, 1197; (e) H. Wamhoff, G. Richardt, and S. Stolben, *Adv. Heterocycl. Chem.*, 1995, **64**, 159.
17. C. Walsh, *Acc. Chem. Res.*, 1986, **19**, 216; and references cited therein.
18. F. Yoneda and K. Tanaka, *Med. Res. Rev.* 1987, **4**, 477; and references cited therein.
19. F. Yoneda and B. Kokel, *Chemistry and Biochemistry of Flavoenzymes*; F. Muller Ed.; CRC Boca Raton, 1991; Vol. 1, pp. 121-169; and references cited therein.
20. F. Yoneda and M. Koga, *J. Chem. Soc., Perkin Trans. I*, 1988, 1813.
21. Y. Tobe, K. Ueda, K. Kakiuchi, Y. Odaira, Y. Kai, and N. Kasai, *Tetrahedron*, 1986, **42**, 1851.
22. A. Altomare, M. C. Burla, M. Camalli, M. Cascarano, C. Giacovazzo, A. Guagliardi, and G. Polidori, *J. Appl. Cryst.*, 1994, **27**, 435.